



ELSEVIER

Mechanics of Materials 33 (2001) 363–370

**MECHANICS
OF
MATERIALS**

www.elsevier.com/locate/mechmat

A micro-mechanics model for imperfect interface in dielectric materials

H. Fan ^{a,*}, K.Y. Sze ^b

^a Center for Mechanics of Micro-systems, School of Mechanical and Production Engineering, Nanyang Technological University, Singapore 639798, Singapore

^b Department of Mechanical Engineering, The University of Hong Kong, Hong Kong SAR, People's Republic of China

Received 1 September 2000; received in revised form 6 November 2000

Abstract

The interface between two dielectric bodies is considered imperfect if there are defects (micro-voids and micro-cracks) present on the interface. For such interface, the perfect continuity condition across the interface is no longer valid and its use in analysis becomes questionable. To account for this imperfection, we propose a micro-mechanics model based on the self-consistent scheme, leading to the establishment of a constitutive relationship between the electric displacement and potential discontinuity across the imperfect interface. © 2001 Elsevier Science Ltd. All rights reserved.

Keywords: Interface; Crack; Dielectric material; Self-consistent scheme

1. Introduction

A perfect interface in dielectric boundary value problems is characterized by the following continuity conditions:

$$\phi^+ = \phi^-, \quad (1.1)$$

and

$$D_2^+ = D_2^- \quad (1.2)$$

along the interface (refer to the coordinate system in Fig. 1(a)). Here ϕ is the electric potential and \mathbf{D} is the electric displacement vector. The super-

scripts “+” and “-” denote $y = 0^+$ and $y = 0^-$, respectively.

As depicted in Fig. 1(b), for an interface with micro-cracks or -voids, the continuity conditions of Eqs. (1.1) and (1.2) are no longer valid. However, if the representative micro-defect size is much smaller than the characteristic dimension of the specimen or the structure, we may merge the micro-cracks along the interface into a continuous damaged interface. For analyses at the structure level, the following condition may be assumed:

$$\overline{D}_2 = k[\overline{\phi}] \quad \text{or} \quad \overline{[\phi]} = \overline{D}_2/k, \quad (1.3)$$

where the bar denotes the average over an area of a scale much greater than the dimension of the micro-cracks. The bracket value of ϕ , $[\phi]$, denotes the discontinuity of ϕ across the interface, namely,

$$[\phi] = \phi^- - \phi^+,$$

* Corresponding author. Tel.: +65-790-4860; fax: +65-791-1859.

E-mail address: mhfan@ntu.edu.sg (H. Fan).

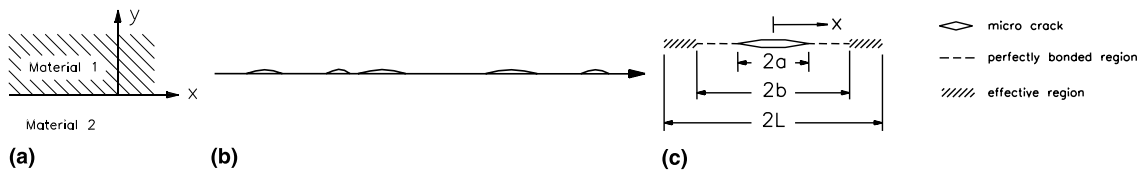


Fig. 1. (a) A bimaterial interface; (b) an imperfect interface with micro-cracks; (c) a self-consistent model for the interface in (b).

where k is dependent on the micro-structure as well as the bi-material properties. For a perfect interface k tends to infinity, while a vanishing k implies the separation of the two bodies. Eq. (1.3) has been referred to as the “spring model” for damaged interfaces.

A few studies on continuous damaged interface have been reported in the literature. Hashin (1991) applied the spring model for the imperfect interface between inclusion and matrix. The author also compiled a list of relevant investigations reported previously. Another group of researchers advocating the interface spring model comes from the non-destructive evaluation society. It has been proved that the interface spring model is easy to use and can explain a certain phenomena observed from the experiments. The analytical results, quoted for comparison with the testing data, were based on either periodically distributed interface cracks (e.g. Margetan et al., 1988) or homogeneous medium due to the mathematical difficulty involved in bi-material interface problem. More related to the present study, Benveniste (1999), Milho and Benveniste (1999) and Benveniste and Milho (1999) used the spring model for the imperfect conductivity interfaces.

The purpose of the present study is to relate the spring constant k of Eq. (1.3) with micro-cracks or -voids along the interface. This relationship is to be sought by applying the so-called “averaging” scheme, which is also known as the micro-mechanics modeling procedure of relating the micro-structure(s) with the macro-constitutive parameters. Such an approach has been widely used in composite mechanics investigation. In fact, a number of micro-mechanics schemes and models have been developed for estimating effective material properties of the composites, such as elastic modulus, dielectric constants and thermal con-

ductivity to name a few (see Christensen, 1990 for a recent review). In the present study, we apply a *generalized self-consistent scheme* of composite mechanics to model imperfect interface between two dielectric bodies. In the following sections, we present discussions which are primarily focused on linear dielectric materials. In terms of the mathematical form, they are read as

$$D_i = \varepsilon_{ij}E_j, \quad (1.4)$$

$$E_i = -\phi_{,i}, \quad (1.5)$$

$$\phi_{,ii} = 0, \quad (1.6)$$

where \mathbf{D} , \mathbf{E} , ε and ϕ are the electric displacement, electric field, permittivity tensor and electric potential, respectively. In Eqs. (1.4)–(1.6), the index summation convention is employed.

2. Self-consistent model for the imperfect interface – plane configuration

This configuration allows us to formulate our model in an analytical form, and highlight the self-consistent scheme. Furthermore, the solution of the singular integral equations based on the model can be compared with the subsequent finite element analysis results.

A schematic representation of an interface under consideration is given in Fig. 1. On the macro level (Fig. 1(a)) the interface is continuous without discrete micro-defects. The continuity condition across the interface follows the spring model (Eq. (1.3)). On the micro-level (i.e. the scale of micro-defects), there are randomly distributed cracks along the interface as shown in Fig. 1(b). A gen-

eralized self-consistent model can be used to equate Fig. 1(b) with (c).

Let us divide the interface into three different regions according to the self-consistent scheme as follows:

- region $-a < x < a$, micro-crack;
- regions $-b < x < -a$ and $a < x < b$, two perfectly bonded regions;
- regions $-L < x < -b$ and $b < x < L$, regions applied the averaging procedure whose properties are unknown yet. Note that a and b are much smaller than L

The continuity or the boundary conditions of these three regions are different. Over the crack surfaces, i.e., $-a < x < a$, we have

$$D_2^+ = D_2^- = 0. \tag{2.1}$$

The electric potential function ϕ has a discontinuity across the interfacial crack. It should be mentioned that different conditions on the interfacial crack surfaces have been used in analytical analyses (Suo et al., 1991). However, no matter which conditions we adopt, the essence of the generalized self-consistent scheme remains the same.

On the other hand, for the perfectly bonded region ($-b < x < -a$ and $a < x < b$), Eqs. (1.1) and (1.2) apply. The effective region ($-L < x < -b$ and $b < x < L$) with continuous damage is described by the spring model of Eq. (1.3).

For the derivation of the governing equations based on the self-consistent micro-mechanics model, a new quantity, the *electric potential jump density*, $h(x)$, is introduced

$$h(x) \equiv \frac{\partial[\phi]}{\partial x}. \tag{2.2}$$

Over the three regions as defined above, the average potential discontinuity can be written by

$$\overline{[\phi]} = \frac{1}{2L} \int_{-L}^L [\phi] dx = \frac{1}{2b} \int_{-a}^a [\phi] dx \tag{2.3}$$

with $[\phi] = 0$ at $x = -a$ and a , the above expression may be written as, via integration by parts,

$$\overline{[\phi]} = -\frac{1}{2b} \int_{-a}^a xh(x) dx. \tag{2.3a}$$

By the analogy between the present boundary value problem defined by Eqs. (1.4)–(1.6) and the anti-plane problem in linear elasticity, the governing integral equation is written as

$$\frac{1}{\pi} \int_{-a}^a \frac{h(s) ds}{x-s} + \frac{1}{\pi} \int_{-L}^{-b} \frac{h(s) ds}{x-s} + \frac{1}{\pi} \int_b^L \frac{h(s) ds}{x-s} = -\frac{2D_2^\infty}{C}, \tag{2.4}$$

where

$$C = \frac{2\varepsilon^{(1)}\varepsilon^{(2)}}{\varepsilon^{(1)} + \varepsilon^{(2)}} \tag{2.5}$$

for isotropic dielectric materials.

By carrying out the integration by part and noting that a and b are much smaller than L , we can approximate Eq. (2.4) as follows:

$$\int_{-1}^1 \frac{h(t) dt}{\xi-t} - \frac{\overline{[\phi]}}{b} \left(\frac{1}{1+\rho\xi} - \frac{1}{1-\rho\xi} \right) = -\frac{2\pi D_2^\infty}{C}, \tag{2.6}$$

where $\rho = a/b$. The non-dimensional coordinates are

$$\xi = x/a \quad \text{and} \quad t = s/a.$$

Eqs. (2.3a) and (2.6) constitute a generalized self-consistent description to the problem. The average electric potential, $\overline{[\phi]}$, is computed from $h(x)$. According to Eq. (2.3a) however the solution of Eq. (2.6) (for $h(x)$) requires the knowledge of the averaged potential, $\overline{[\phi]}$.

By substituting $\overline{[\phi]}$ given by Eq. (2.3a) into Eq. (2.6), we have an integral equation for $h(x)$ with the first term having a Cauchy-type kernel and the second term with a non-singular kernel. The solution of this singular integral equation can be obtained numerically by using, say, Erdogan's scheme (Erdogan, 1975). Before discussing the numerical solution, we first present an analytical approximate solution valid for $\rho \ll 1$ which is obtained by neglecting interactions among the micro-cracks. The approximate solution of Eq. (2.6) is found in a closed form,

$$h(t) = -\frac{2D_2^\infty}{C} (1-t^2)^{-1/2} t. \tag{2.7}$$

By combining the above expression with Eqs. (2.2) and (2.3), one has

$$\overline{[\phi]} = -\frac{a\rho}{2} \int_{-1}^1 th(t) dt = \frac{a\pi\rho D_2^\infty}{2C}. \quad (2.8)$$

Comparing Eq. (2.8) with Eq. (1.3), the following result is obtained:

$$k = \frac{2C}{\pi} \frac{1}{\rho}. \quad (2.9)$$

For interfaces with large ρ , a numerical scheme, say Erdogan (1975), is required, with which the solution of whole range of ρ is obtained.

In the present study, instead of using the singular equation approach, we employed finite element method to carry out the numerical calculations. The stability and reliability of the commercial FEM package, ABAQUS (1998), shows great advantage over the solution scheme via the formulation of Erdogan (1975) for singular integral equation. It has been noted that the finite element method for solving this kind of mixed-boundary value problem has substantial advantage for problems where the singularities are changing (Fan et al. (2000)).

Fig. 2 shows the system used for the finite element calculations. The spatial domain consists of two $2L \times h$ dissimilar dielectric materials with the

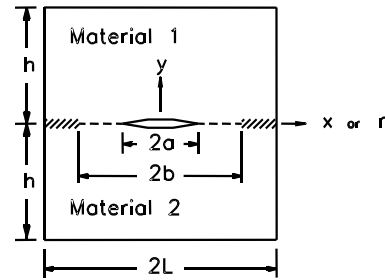


Fig. 2. Problem domain for finite element solutions. Problem parameters: $b = 1, h = L = 15, \epsilon^{(1)} = 1, a$ and $\epsilon^{(2)}$ are varied.

interface at $y = 0$. For the calculation, we fixed certain parameters. They are $b = 1, h = L = 15$ and $\epsilon^{(1)} = 1$ whereas a and $\epsilon^{(2)}$ will be varied. The prescribed boundary conditions were: $D_y = q = 1$ at $y = \pm h$ and $D_x = 0$ at $x = \pm L$. At the interface, the governing conditions were:

- (i) $D_y = 0$ over the micro-crack ($-a < x < a$);
- (ii) $[\phi] = 0$ over the perfectly bonded region ($-b < x < -a$ and $a < x < b$);
- (iii) $k[\phi] = q$ over the effective region ($-L < x < -b$ and $b < x < L$) and, most importantly;
- (iv) $k[\phi] = q$ over the micro-crack and perfectly bonded region ($-b < x < b$).

Owing to symmetry, only $x \geq 0$ is modeled and the commercial finite element software ABAQUS

Table 1
Computed ka/C for plane configuration

a/b	$\epsilon^{(2)}$						
	1	5	10	50	100	500	1000
0.02	35.91	35.93	35.90	35.93	35.90	35.93	35.92
0.032	21.45	21.45	21.44	21.45	21.43	21.43	21.44
0.05	13.37	13.33	13.35	13.35	13.36	13.36	13.35
0.07	9.396	9.406	9.413	9.395	9.402	9.402	9.405
0.1	6.494	6.522	6.494	6.497	6.499	6.498	6.496
0.14	4.590	4.590	4.589	4.592	4.588	4.590	4.589
0.2	3.175	3.166	3.165	3.163	3.165	3.165	3.164
0.3	2.048	2.045	2.045	2.045	2.045	2.045	2.044
0.4	1.473	1.472	1.472	1.472	1.471	1.471	1.471
0.5	1.111	1.111	1.111	1.111	1.112	1.112	1.111
0.6	0.8571	0.8571	0.8558	0.8550	0.8554	0.8554	0.8551
0.7	0.6542	0.6542	0.6547	0.6547	0.6544	0.6544	0.6541
0.8	0.4819	0.4819	0.4819	0.4815	0.4819	0.4819	0.4817
0.9	0.3125	0.3121	0.3123	0.3120	0.3122	0.3122	0.3121

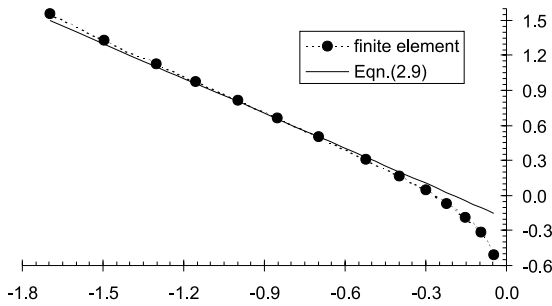


Fig. 3. Log(ka/C) versus log(a/b) for plane configuration obtained by finite element computation and Eq. (2.9).

(1998) is resorted to. While it is straightforward to prescribe (i) and (ii), (iii) for any k can be enforced by using the linear constraint equation facility available in ABAQUS and (iv) cannot be prescribed or enforced by any direct means. Thus, we vary k in the linear constraint equation until the following 0.5% tolerance condition is met:

$$-0.005 < k\overline{[\phi]}/q - 1 < 0.005, \tag{2.10}$$

where

$$\overline{[\phi]} = \frac{\int_{-b}^b [\phi] dx}{\int_{-b}^b dx} = \frac{1}{b} \int_0^b [\phi] dx = \frac{1}{b} [\phi] dx.$$

Regarding the finite element mesh, around 10,000 four-node plane elements are employed with the highest element densities arranged at $(x = a, y = 0)$ and $(x = b, y = 0)$ so that the associated electric flux concentration can be accurately captured. It has been checked by including more elements into the mesh that the latter has been fine enough to secure sufficiently accurate predictions. Table 1 lists the computed ka/C by varying a/b and the permittivity of the material below $y = 0$. The results are insensitive to $\epsilon^{(2)}$ or C ($= 2\epsilon^{(1)}\epsilon^{(2)}/\epsilon^{(1)} + \epsilon^{(2)}$). The finite element results together with Eq. (2.9) are shown in Fig. 3.

3. Three-dimensional configuration

For the three-dimensional configuration, the finite element method is again adopted. The finite element model is built upon the assumption that

the three-phase-model forms an axial symmetric configuration as shown in Fig. 2. The problem parameters, boundary and interfacial conditions are essentially the same as the plane case except that x becomes r and r must be positive. Moreover, the area average of the electric potential discontinuity with 0.5% tolerance condition in (2.10) has to be amended as

$$\begin{aligned} \overline{[\phi]} &= \frac{\int_0^b 2\pi r [\phi] dr}{\int_0^b 2\pi r dr} = \frac{2}{b^2} \int_0^b r [\phi] dr \\ &= \frac{2}{b^2} \int_0^a r [\phi] dr. \end{aligned}$$

Using the same mesh for the plane configuration built by four-node axisymmetric elements, Table 2 lists the computed ka/C , by varying a/b and the permittivity of the material below $y = 0$. Again, the results are insensitive to $\epsilon^{(2)}$ or C . Fig. 4 shows the log–log plot for ka/C against a/b . Similar to Fig. 3, the relation is linear for small a/b .

4. Interface between anisotropic bodies

It is simple to extend the finite element method described in the previous sections to interfaces between two anisotropic dielectric bodies. The normalization constant C which appeared in the numerical result does require further treatment. To determine this constant C , we followed the procedure of the so-called Stroh formalism that has been widely applied in linear anisotropic elasticity studies (Ting, 1995). The notation used before (Fan, 1994, 1995) will be adopted here.

Let us start with a two-dimensional dielectric boundary value problem for general anisotropic materials, the governing equations are:

$$D_i = \epsilon_{ij} E_j, \tag{4.1}$$

$$E_i = -\phi_{,i}, \tag{4.2}$$

$$D_{i,i} = 0. \tag{4.3}$$

We can assume that the potential, ϕ , can be considered as a function of a single complex variable:

$$\phi = f(z) = f(x + py) \tag{4.4}$$

Table 2
Computed ka/C for axisymmetric configuration

a/b	$\epsilon^{(2)}$						
	1	5	10	50	100	500	1000
0.02	3530	3530	3530	3531	3529	3531	3531
0.032	1290	1289	1289	1289	1289	1290	1290
0.05	507.6	508.5	509.3	507.5	505.0	506.1	507.6
0.07	253.6	253.8	253.8	253.7	253.6	253.6	253.5
0.1	122.0	122.4	122.2	122.6	122.3	122.2	122.4
0.14	61.81	61.76	61.80	61.82	61.75	61.80	61.79
0.2	30.08	30.00	30.05	30.00	29.88	29.91	29.97
0.3	13.10	13.14	13.10	13.12	13.17	13.10	13.11
0.4	7.273	7.273	7.261	7.247	7.266	7.245	7.248
0.5	4.505	4.478	4.508	4.505	4.477	4.489	4.493
0.6	2.970	2.951	2.973	2.971	2.971	2.964	2.963
0.7	2.012	2.000	2.005	1.994	2.009	2.004	2.002
0.8	1.333	1.326	1.333	1.340	1.338	1.332	1.332
0.9	0.7895	0.7918	0.7920	0.7914	0.7904	0.7911	0.7903

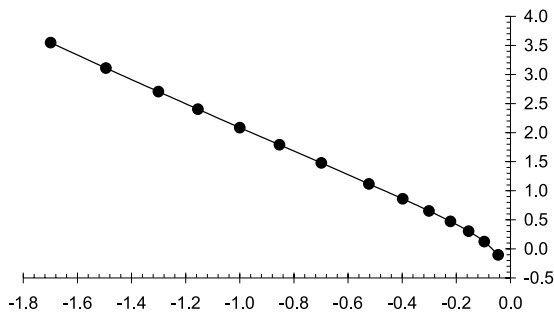


Fig. 4. $\log(ka/C)$ versus $\log(a/b)$ for axisymmetric configuration obtained by finite element computation.

where p is a complex number. By substituting Eq. (4.4) into Eq. (4.1), the equivalent of Eq. (4.3) is

$$(\epsilon_{11} + 2p\epsilon_{12} + p^2\epsilon_{22})\phi'(z) = 0. \tag{4.5}$$

For a non-zero solution of ϕ , one must have

$$\epsilon_{11} + 2p\epsilon_{12} + p^2\epsilon_{22} = 0. \tag{4.6}$$

The two roots of this equation are:

$$p = -\frac{\epsilon_{12}}{\epsilon_{22}} + i\sqrt{\frac{\epsilon_{11}}{\epsilon_{22}} - \left(\frac{\epsilon_{12}}{\epsilon_{22}}\right)^2}$$

and

$$\bar{p} = -\frac{\epsilon_{12}}{\epsilon_{22}} - i\sqrt{\frac{\epsilon_{11}}{\epsilon_{22}} - \left(\frac{\epsilon_{12}}{\epsilon_{22}}\right)^2} \tag{4.7}$$

It is noted that the p must be a complex number because the permittivity tensor, ϵ , is positive definite. In the case of isotropic bodies, $p = i$ and $-i$.

With the complex function $f(z)$, the potential and electric displacement may be rewritten as

$$\phi = 2\text{Re}(f(z)) = f(z) + \overline{f(z)}, \tag{4.8}$$

$$D_2 = -2\text{Re}(Lf'(z)), \tag{4.9}$$

where the bar denotes the complex conjugate in this section, and

$$L = \epsilon_{2j}(\delta_{1j} + p\epsilon_{2j}) = i\sqrt{\epsilon_{11}\epsilon_{22} - (\epsilon_{12})^2}. \tag{4.10}$$

Accordingly, the electric displacement continuity condition of Eq. (1.2) along the interface $y = 0$ is

$$L_1f_1'(x) + \overline{L_1f_1'(x)} = L_2f_2'(x) + \overline{L_2f_2'(x)}, \tag{4.11}$$

where the subscripts 1 and 2 refer to the upper body and the lower body, respectively. Eq. (4.11) implies that

$$L_1f_1'(z) = \overline{L_2f_2'(\bar{z})} \quad \text{for } y > 0, \tag{4.12a}$$

$$\overline{L_1f_1'(\bar{z})} = L_2f_2'(z) \quad \text{for } y < 0. \tag{4.12b}$$

With all these in our mind, we may have the potential discontinuity condition along the interface $y = 0$ as

$$-i[\phi'] = HL_1 f_1'(x) - \overline{H}L_2 f_2'(x), \tag{4.13}$$

where

$$H = i(L_1^{-1} - \overline{L_2^{-1}}). \tag{4.14}$$

Analogous to dislocation in linear elastic solids (Fan, 1994), we have

$$L_1 f_1(z) = \overline{L_2 f_2(\bar{z})} = -\frac{1}{2\pi} H^{-1} [\phi] \ln z. \tag{4.15}$$

Therefore the electric displacement along the interface can be obtained from Eq. (4.9) as

$$D_2 = \frac{1}{2\pi} (H^{-1} + \overline{H}^{-1}) \frac{[\phi]}{x}. \tag{4.16}$$

By substituting the H by Eqs. (4.14) and (4.10), we have

$$\begin{aligned} H^{-1} + \overline{H}^{-1} &= 2H^{-1} \\ &= \frac{2\sqrt{\varepsilon_{11}^{(1)}\varepsilon_{22}^{(1)} - (\varepsilon_{12}^{(1)})^2} \sqrt{\varepsilon_{11}^{(2)}\varepsilon_{22}^{(2)} - (\varepsilon_{12}^{(2)})^2}}{\sqrt{\varepsilon_{11}^{(1)}\varepsilon_{22}^{(1)} - (\varepsilon_{12}^{(1)})^2} + \sqrt{\varepsilon_{11}^{(2)}\varepsilon_{22}^{(2)} - (\varepsilon_{12}^{(2)})^2}}. \end{aligned} \tag{4.17}$$

It is seen that Eq. (4.17) becomes the constant C stated in Eq. (2.5) when both of the materials are isotropic, where $\varepsilon_{11} = \varepsilon_{22}$ and $\varepsilon_{12} = 0$. In other words, the numerical results for the interface between two anisotropic materials will be normalized by the constant defined by Eq. (4.17).

5. Discussion and conclusions

In Fig. 3, the finite element numerical result for the plane configuration case is compared with Eq. (2.9) which is solved via the singular equation scheme without considering the interaction among the micro-cracks along the interface. It is seen that the non-interaction solution Eq. (2.9) can be applied up to $\rho = a/b = 0.3$ with less than 5% deviation from the finite element results listed in Table 1.

For the three-dimensional configuration, we studied the case of isotropic damaged interface.

The isotropic assumption leads the axial symmetry configuration for our numerical analysis. It is needless to say that there is a derivation of the three-dimensional problem via the singular integral equation approach where elliptical function will be involved. With verified finite element analysis in plane configuration, the same mesh and procedure is applied to the axial symmetry in ABAQUS. Comparing Figs. 3 and 4, we see a similar trend for the two-dimensional interface and three-dimensional interface in terms of the “spring constant”.

It is realized that there are other engineering problems which are described by the same set of governing equations as the dielectric problem. For example, the temperature distribution function of steady heat conduction problem obeys the Laplace equation Eq. (1.6) together with proper boundary conditions. Therefore, we can expect the imperfect interface in the heat conduction problem to be modeled via the same scheme. Another problem which belongs to the same category is the imperfect interface in linear elasticity under anti-plane condition, which can be treated by the present model. Readers may realize this during the reading of our previous sections since we have borrowed the formulation and solutions from the linear elasticity.

Lastly, we would like to mention that the present boundary value problem under the self-consistent scheme is posted on a two-dimensional surface (interface), while the original self-consistent scheme was developed on the three-dimensional solids. It is not a simple reduction of dimensions. Rather, the level of the complexity in our self-consistent model on the two-dimensional surface is higher than the original one, because the present model is described by a singular integral equation in nature. Sometimes, it is called the mixed boundary value problem (Erdogan, 1975).

Acknowledgements

Part of the study reported here was carried out during the first author’s stay at the University of Hong Kong as a William Mong Visiting Research Fellow.

References

- ABAQUS, 1998. The user manual, Version 5.8. Hibbitt, Karlsson & Sorensen, RI, USA.
- Benveniste, Y., 1999. On the decay of end effects in conduction phenomena: a sandwich strip with imperfect interfaces of low or high conductivity. *J. Appl. Phys.* 86 (3), 1273–1279.
- Benveniste, Y., Milho, T., 1999. Neutral inhomogeneities in conduction phenomena. *J. Mech. Phys. Solids* 47, 1873–1892.
- Christensen, R.M., 1990. A critical review for a class of micro-mechanics models. *J. Mech. Phys. Solids* 38 (3), 379–404.
- Erdogan, F., 1975. Mixed boundary value problems in mechanics. In: S. Nemat-Nasser (Ed.), *Mechanics Today*, pp. 1–86.
- Fan, H., Han, Z., Sze, K.Y., 2000. Micro-mechanics modeling for asperity contact. *Mech. Mater.* (submitted).
- Fan, H., 1995. Decay rates in a piezoelectric strip. *Int. J. Eng. Sci.* 33 (8), 1095–1103.
- Fan, H., 1994. Interfacial Zener–Stroh crack. *ASME J. Appl. Mech.* 61 (4), 829–834.
- Hashin, Z., 1991. The spherical inclusion with imperfect interface. *ASME J. Appl. Mech.* 58 (3), 444–449.
- Margetan, F.J., Thompson, R.B., Gray, T.A., 1988. Interfacial spring model for ultrasonic interactions with imperfect interfaces. *J. Nondestructive Evaluation* 7 (3/4), 131–152.
- Milho, T., Benveniste, Y., 1999. On the effective conductivity of composites with ellipsoidal inhomogeneities and high conducting interface. *Proc. R. Soc. Lond. A* 455, 2687–2706.
- Suo, Z., Kuo, C.M., Barnett, D.M., Willis, J.R., 1991. Fracture mechanics for piezoelectric ceramics. *J. Mech. Phys. Solids* 40, 739–765.
- Ting, T.C.T., 1995. *Anisotropic Elasticity*. Oxford University Press, UK.